



Assessing shear wave velocity profiles using multiple passive techniques of Shillong region of northeast India

Rajib Biswas¹ · S. Baruah² · Nilutpal Bora¹

Received: 18 July 2016 / Accepted: 13 August 2018 / Published online: 17 August 2018
© Springer Nature B.V. 2018

Abstract

Shillong region of northeast India falls under seismic zone V. Being a commercial hub, urbanization in this study region is at its peak. In order to qualitatively assess the sub-surface velocity profiling of this area, we have blended two robust techniques, namely spatial autocorrelation (SPAC) and frequency wavenumber (FK) method. Corresponding to array noise data collected at five sites, situated in the close proximity of boreholes, we have evaluated V_S and V_P as well. The shear wave velocity estimates yielded by these techniques are found to be consistent with each other. The computed V_S values up to depth of 30 m are observed to be in the range of 275–375 m/s, in most of the sites which implies prevalence of low-velocity zone at some pocket areas. The estimates so found are systematically analyzed and implications are outlined. The results were corroborated by substantial evidence of site geology as well as geotechnical information.

Keywords Array recordings · SPAC · Frequency wave number technique · Shear wave

1 Introduction

Microtremors play an important role in effective evaluation of site effects. Because of their ready availability and easy handling, they are preferred over earthquakes. Recording earthquakes and maintenance of equipment thereafter are time-consuming and expensive, as compared to seismic noise. The information relating subsurface elastic properties toward prediction of site effect from seismic noise acts as a prominent factor for seismic hazard assessment (Hartzell et al. 1996; Yamanaka et al. 1993, 1994; Yamanaka 1998; Köhler et al. 2007, Papadopoulou-Vrynioti et al. 2013; Pavlou et al. 2013; Kassaras et al. 2015). These

Electronic supplementary material The online version of this article (<https://doi.org/10.1007/s11069-018-3453-2>) contains supplementary material, which is available to authorized users.

✉ Rajib Biswas
rajib@tezu.ernet.in

¹ Geophysical Lab, Department of Physics, Tezpur University, Napaam, Tezpur, Assam 784028, India

² Geoscience Division, C.S.I.R-North East Institute of Science and Technology, Jorhat, Assam 785006, India

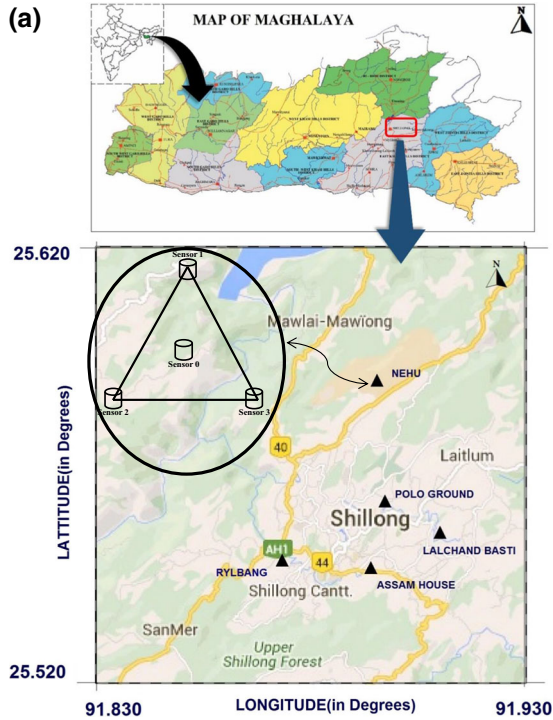
Fig. 1 **a** Locations of the five array sites in Shillong city which is represented by the filled triangles. In inset, map of India is given along with the study area in Meghalaya state. Deployed pattern of array layout is indicated inside the circle connected to one of the stations. **b** Geological map of Shillong city (after GSI 1985). The scale shown in the figure is in kilometers

site effects are found to be explicitly frequency dependent which is characterized by shear wave velocity of the subsurface structure. Shear wave velocity is regarded to be very much influential in ground motion amplification (Borcherdt 1970; Campbell 1976; Ohnberger et al. 2004a), leading to greater extent of damage in populated areas which are basically situated on sedimentary areas (Ohnberger et al. 2004b; Wathelet et al. 2005). Due to the dispersive character of shear wave velocity, it can be exploited to reveal underlying velocity structure (Williams et al. 2003). Utilization of microseism data attained from array of sensors has already been proven to be effective in computing shear wave velocity. Recently, Biswas and Baruah 2011 estimated the site effect of Shillong area through modified method of Nakamura. More specifically, Biswas et al. (2013a, b) analyzed effect of attenuation and site effect in Shillong area using microtremors. Again in the same region, mapping of sediment thickness has been accomplished by Biswas et al. (2015a). Similarly, nonlinear earthquake site response analysis in Shillong region has also been executed (Biswas and Baruah 2015b). Again, frequency dependent microtremor estimation of Shillong region was done recently by Biswas et al. 2018. Toward estimations of shear wave velocity structure, spatial autocorrelation (Okada 2006) and frequency wave number method (Kvaerna and Ringdahl 1986) are very much effective. There are reports of successful implementation of these techniques to decipher shear wave velocity (Fäh et al. 2003; Picozzi et al. 2005; Di Giulio et al. 2006; Claprod and Asten 2007a, b, 2010; Biswas and Baruah 2016). Of late, the seismic activity of Shillong region has risen. Thanks to the instrumental records of large no. of felt earthquakes. Situated in a tectonically active area, the region is prone to seismic hazard. As such, assessment of velocity profiles pertinent to this area is the need of the hour which will act as a vital role for geo-engineers and policy makers toward mitigation of seismic hazard.

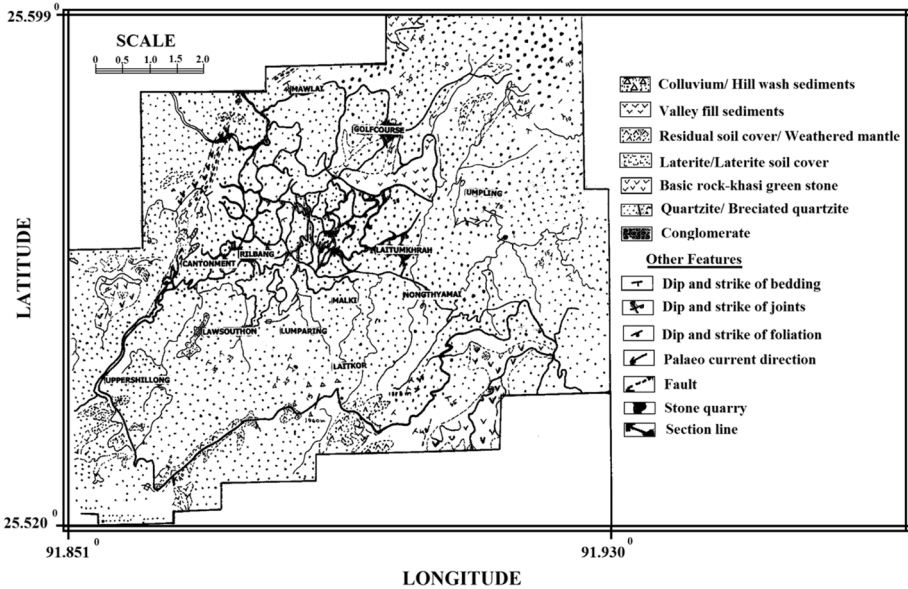
Keeping this in mind, we have made an attempt to exploit SPAC and FK approach to have a reliable estimate of velocity to depth profile. Here, we have first derived autocorrelation curves through spatial autocorrelation technique and then subsequently inverted them to obtain the velocity to depth profiles. Similarly, we have also performed shear wave velocity modeling after inversion of dispersion curves attained through frequency wave number technique. Furthermore, we have compared our results with available geophysical data. Again, the one-dimensional velocity models are analyzed in terms of frequency band. Finally, we have made a cross-check of attained velocity models to empirical shear wave velocity estimates, aided by good coverage of geotechnical parameters.

2 Geological settings of Shillong

Shillong city, with an area coverage of 6430 square kilometer and average elevation of 1000 m, has an approximate population of $\sim 2,00,000$. Situated in Shillong Plateau (SP), the greater part of Shillong is characterized by an Archean gneissic basement and late Cretaceous–Tertiary sediments along its southern margin (Kayal et al. 2006; Kayal 2008; Rao and Rao 2008). Presence of Shillong series of parametamorphites, including mostly quartzites and sandstones, is a feature of this region. There are also schist, phyllites, slates, etc. The major constituent of Shillong series is attributed to Archean crystalline which is again overlain by Shillong series of rocks as sedimentary deposits (Mitra and Mitra 2001; Sar 1973). There is an intrusion of epidiorite rocks, known as Khasi Greenstone, as outlined in Fig. 1b (Srinivasan et al. 1996, Chattopadhaya and Hashimi 1984). The



(b) GEOLOGICAL MAP OF GREATER SHILLONG AREA, EAST KHASI HILLS DISTRICT, MEGHALAYA



topographically depressed areas are actually populated by these highly weathered rocks. Meanwhile, there is copious amount of valley fill sediments in low lying areas.

3 Generation of data

In this work, we designed an array consisting of four sensors, laid out at five selective locations which were in close vicinity to boreholes in Shillong city. We implemented equilateral triangular array with three sensors laid out at the vertices while the fourth sensor was placed at the in center of the triangle. The radius was kept at 10 m. For each of the cases, a homogeneous instrumentation was implemented with good soil sensor coupling. It comprised of three Kinemetrics Trillium 120P sensors and one short period S-13 from Teledyne Geotech. Each station was synchronized by GPS receivers. Data were digitized at 100 samples per sec. The ambient noise wave fields from array radius of 10 m were the prime input toward estimation of velocity profile. Accordingly, the aperture is kept at a value 17 m. The outlined circle in Fig. 1a shows the adopted layout in selective locations in Shillong city.

The arrays with similar configuration were deployed at locations, viz. ASSAM HOUSE, POLO GROUND, NEHU, LALCHAND BASTI and RYLBANG, as demonstrated in Fig. 1a. The locations of these array sites are provided in Table 1. The array transfer function, as proposed by Woods and Lintz (1973), is defined in the wave number limits k_{\min} and k_{\max} and is described in the k_x and k_y plane. The corresponding theoretical array response is represented in Fig. 2. After obtaining array noise records, they were pre-processed, as detailed in SESAME (2004), in order to make them fit for two distinctive computing techniques: SPAC and FK in this study.

4 Theoretical formulation

4.1 Spatial autocorrelation method

The spatial autocorrelation technique exploits random distribution of sources in time and space, linking autocorrelation ratios to phase velocities. In case of a single-valued phase velocity per frequency band, Aki (1957) showed that these ratios have the shape of zero-order Bessel functions, the argument of which is dependent upon the dispersion curve values and array aperture actually effect the argument of the ratios. Meanwhile, some revisions were incorporated by Bettig et al. (2001) to fit it for irregular arrays.

The spatial autocorrelation function of the single plane wave polarized in x direction, $u(x, t)$ for the region $x \in [0, X]$ and the time domain $t \in [0, T]$ is defined as follows after Wathelet et al. (2004).

Table 1 Locations of array sites

Station Name	Latitude (°)	Longitude (°)	Elevation (m)
ASSAM HOUSE	25.567	91.892	1544
LALCHAND BASTI	25.590	91.915	1456
RYLBANG	25.574	91.880	1562
NEHU	25.611	91.901	1427
POLO GROUND	25.580	91.888	1444

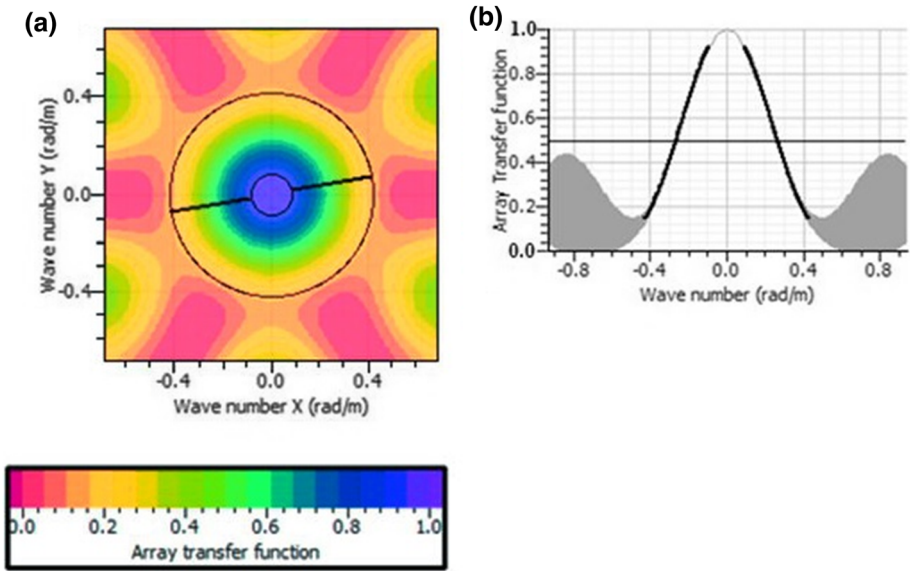


Fig. 2 Theoretical array response for the adopted array layout. **a** Array responses computed for the whole band of frequency. k_x and k_y are values are plotted along the horizontal and vertical axis, respectively. The color scale indicates the values of array transfer function. **b** Plot of array transfer function versus wave number. The single peak appearing here corresponds to the main peak. The other side lobes represent the aliasing peaks

$$\langle \phi(\xi, t) \rangle_x = \frac{1}{X} \int_0^X u(x, t) u(x + \xi, t) dx \tag{1}$$

Equation (1) can be expressed as,

$$\phi(\xi) = \langle \phi(\xi, t) \rangle_x = \frac{1}{T} \int_0^T v_0(t) v_\xi(t) dt \tag{2}$$

where $v_0(t) = u(x_0, t)$ and $v_\xi(t) = u(x_0 + \xi, t)$ are related to signals recorded at two stations separated by distance ξ .

The autocorrelation function can also be expressed in the following form after Aki (1957)

$$\phi(\xi) = \frac{1}{\pi} \int_0^\infty \phi(\omega) \cos\left(\frac{\omega}{c(\omega)} \xi\right) d\omega \tag{3}$$

where $\phi(\omega)$ is the autocorrelation frequency spectrum; ω is the angular frequency; and $c(\omega)$ is the frequency-dependent velocity. If the power spectral density is designated by $P(\omega_0)$ for a narrow band filter centered at ω_0 and Dirac function by δ , then it follows

$$\phi(\omega) = P(\omega_0) \delta(\omega - \omega_0) \tag{4}$$

so that Eq. (4) changes to

$$\phi(\xi, \omega_0) = \frac{1}{\pi} P(\omega_0) \cos\left(\frac{\omega_0}{c(\omega_0)} \xi\right) \tag{5}$$

The spatial autocorrelation ratio $\rho(\xi, \omega)$ can also be expressed as

$$\rho(\xi, \omega_0) = \frac{\phi(\xi, \omega_0)}{\phi(0, \omega_0)} \tag{6}$$

Using Eqs. (5) and (6), we arrive at

$$\rho(\xi, \omega_0) = \cos\left(\frac{\omega_0}{c(\omega_0)} \xi\right) \tag{7}$$

This relationship given by Eq. (7) yields dispersion curve when it is inverted. For an unknown propagating waveform, Eq. (7) can be modified a little bit wherein the distance and azimuth between the stations are incorporated. Equation (7) changes to

$$\rho(r, \varphi, \omega_0) = \cos\left(\frac{\omega_0 r}{c(\omega_0)} \cos(\theta - \varphi)\right) \tag{8}$$

where r and φ correspond to distance and azimuth of direction between stations, while θ refers to azimuth of propagating seismic ambient noise. It is quite evident from Eq. (8) that ρ constantly decreases with increment in frequency along the propagation direction ($\varphi = \theta$) and then ideally, it becomes constant along the wave front ($\varphi = \theta \pm \pi/2$). Practically, there is little information about θ . As a result, an azimuthally averaged autocorrelation ratio is introduced to take care of the uncertainty in the case of θ .

$$\rho(r, \varphi, \omega_0) = \frac{1}{\pi} \int_0^\pi \rho(r, \omega_0) d\varphi \tag{9}$$

Then, for a wave filtered around ω_0 , using Eq. (9), it is obtained as

$$\overline{\rho(r, \omega_0)} = J_0\left(\frac{\omega_0 r}{c(\omega_0)}\right) \tag{10}$$

where J_0 is the Bessel function of zero order, $J_0(x) = \frac{1}{\pi} \int_0^\pi \cos(x \cos(\varphi)) d\varphi$

For a real array suffering from topographic irregularities, the modified ratio is

$$\overline{\rho_{r_1, r_2}}(\omega) = \frac{2}{\pi(r_2^2 - r_1^2)} \int_0^\pi \int_{r_1}^{r_2} \rho(r, \varphi, \omega) r dr d\varphi \tag{11}$$

Adopting the aforementioned theoretical procedure, we computed each spectrum pertaining to the array sites, deployed at those selective locations with window size of ten minutes. Accordingly, we have evaluated spatial autocorrelation ratio for the respective five sites. Through Eq. (9), we computed spatial autocorrelation ratios for each respective site. During computation of spatial autocorrelation ratios, we maintained spatial coherency of ambient noise records. For each respective array site, the SPAC curves for deriving shear wave velocity were attained ensuring proper coherency of ambient noise records. Figure 3a depicts the autocorrelation ratio obtained for one of the sites. These attained

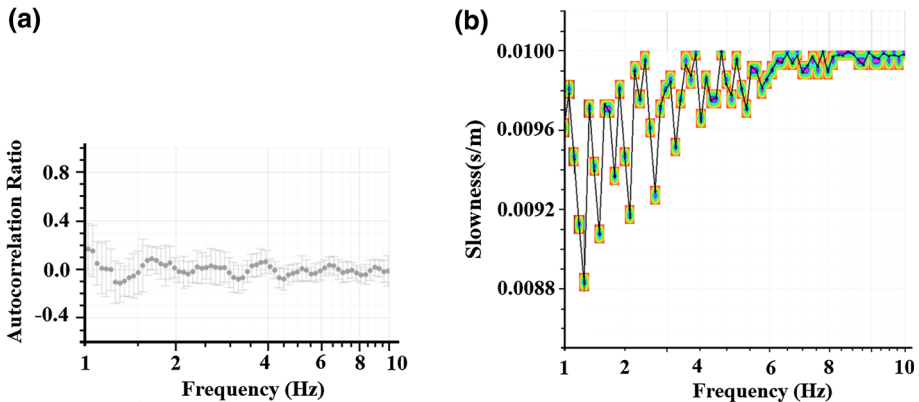


Fig. 3 **a** Spatial autocorrelation curves for one of the sites. **b** FK dispersion curves for the same site

SPAC curves are checked for consistency and are inverted for derivation of shear wave velocity profile.

4.2 Frequency wave number technique

Furthermore, we adopt frequency wave number technique in order to exploit the plane wave approach of propagating noise wavefield which is quite different from SPAC. Here, the most coherent plane wave provides the propagation characteristics in terms of horizontal slowness and azimuth (Seligson 1970). While measuring the wave propagation characteristics, the appropriate frequency bands are explored in the engineering range of frequencies (Bozdag and Kocaoglu 2005). The lower frequency of analysis is provided by the eigen frequency of the sensors. In the similar fashion, the upper frequency is fixed by spatial aliasing determined by k_{\max} and k_{\min} .

For this particular study, window length is chosen on the basis of central frequency of the analyzed frequency band. In order to acquire effective sampling, an additional overlap of 50% is incorporated. This has been done to augment number of analyzed windows having the duration of 10–20 s. Subsequently, the velocity structure could be modeled by inverting dispersion curve at each site. The noise data collected at array sites were initially subjected to Fourier amplitude spectra analysis in order to have an inspection of the quality of the data for all array stations. The dispersion curve for each array was computed with 10 min of noise recording, like SPAC. However, it is worthwhile to note that the frequency range where the reliability of the dispersion curve depends is totally controlled by the effective wavelengths contributing to the wave field and the limitations induced by the array geometry. In this work, the beam forming method has been exploited to compute the dispersion curve (Bozdag and Kocaoglu 2005). The dispersion curves are estimated at each of the array sites which are inverted to obtain respective depth to velocity profile. As for instance, Fig. 3b shows dispersion curve for one of the sites. After obtaining the dispersion curves through these, we intend to derive shear wave velocity models, accompanied by V_p values at these five array sites. While doing so, as input parameter for the required modeling, we enlist the values of three sites in Tables 2, 3 and 4, respectively, in synchrony with the available borehole information. For the other two sites, where no prior information was available regarding depth, the inversion is confined to depth of 30 m only,

Table 2 Parameterized model for inversion up to depth of 65 m

Layer	Thickness (m/s)	V_P (m/s)	V_S/V_P	Poisson's ratio	Density (t/m^3)
Sediments	65 m No. of layers 8	200–1275	0.1–0.707	0.2–0.5	2
Half space	–	2000–3000	0.1–0.707	0.2–0.5	2

Table 3 Parameterized model for inversion up to depth of 51 m

Layer	Thickness	V_P (m/s)	V_S/V_P	Poisson's ratio	Density (t/m^3)
Sediments	1–51 m No. of sub layers 5	300–1000	0.1–0.707	0.2–0.5	2
Half space	–	2000–3000	0.1–0.707	0.2–0.5	2

Table 4 Parameterized model for inversion up to depth of 100 m

Layer	Thickness	V_P (m/s)	V_S/V_P	Poisson's ratio	Density (t/m^3)
Sediments	1–100 m No. of sub layers 5	450–1475	0.1–0.707	0.2–0.5	2
Half space	–	2250–4200	0.1–0.707	0.2–0.5	2

as given in Table 5. Thus, we have attained velocity models for all the five array sites by inverting the dispersion curves of SPAC and FK with the aid of modified neighborhood algorithm (Sambridge 1999a, b) by Wathelet et al. (2004). The inversion results from SPAC and FK dispersion curves are detailed below separately.

5 Results from SPAC and frequency wave number technique and their interpretation

The site-specific shear wave velocity models attained by means of SPAC and FK analysis are detailed below.

Table 5 Parameterized model for inversion for an arbitrary depth of 30 m

Layer	Thickness	V_P (m/s)	V_S/V_P	Poisson's ratio	Density (t/m^3)
Sediments	30 m No. of layers 6	200–1000	0.1–0.707	0.2–0.5	2
Half space	–	2000–3500	0.1–0.707	0.2–0.5	2

5.1 ASSAM HOUSE

5.1.1 From SPAC

The compressional wave- V_P and shear wave- V_S profile computed for this site are demonstrated in Fig. 4(i)a. The depth of the profile is restricted to 30 m, so as to obtain relevant information due to lack of a priori information of local geology. The shear wave velocity is found to vary between 200 and 400 m/s up to depth of 30 m corresponding to the lowest misfit. There is gradual increase observed in V_S from 1 m depth. Corresponding to 1 m stratum of top layer, the shear wave velocity has been estimated to be 220 m/s, whereas the V_P value is found to be 500 m/s. In the intermediate layers having thickness of 2 and 4 m, the V_S values are found to be 260 m/s and 310 m/s, respectively. The bottom layer whose thickness is 14 m yields the highest value of shear wave velocity of 430 m/s.

5.1.2 From FK

In case of this site, the V_S profile shows variation from 200 to 415 m/s, as illustrated in Fig. 4(i)b. Simultaneously, the V_P values vary between 500 and 705 m/s. In conformity with SPAC inversion, here also the depth up to which inversion is carried out is confined to 30 m due to lack of a priori information on depth. The uppermost layer is found to have a shear wave velocity of 215 m/s, whereas V_P is estimated to be 500 m/s. The deeper layers show gradual increase in shear wave velocities; same is the case with estimates of V_P values as well.

5.2 NEHU

5.2.1 From SPAC

This site like the ASSAM HOUSE is a plain land formation but with nearest borehole information. As such, litholog information toward direct inversion of SPAC curves can be incorporated. So far the velocity profiles are concerned; the depth, up to which profile has been confined up to 55 m, is illustrated in Fig. 4(ii)a. As evident in the figure, the surface layer having thickness of 8.5 m produces a very low value of V_S which has been estimated to be 120 m/s resulting from this inversion. As for the V_P , it is found at 390 m/s. Toward deeper formation of layers, the shear wave velocity is observed to be slowly rising, reaching a value of 210 m/s for the bottom layer. The same trend is observed to hold for the estimates of V_P values. Summarily, these results indicate a low-velocity zone pertinent to this site.

5.2.2 From FK

Figure 4(ii)b shows the inversion results of site NEHU. The V_S is found within the range of 200–500 m/s, while the V_P exhibits a variation of 625–1200 m/s. The shear wave model produced by the inversion also shows a linear increase in velocity with rise in depth.

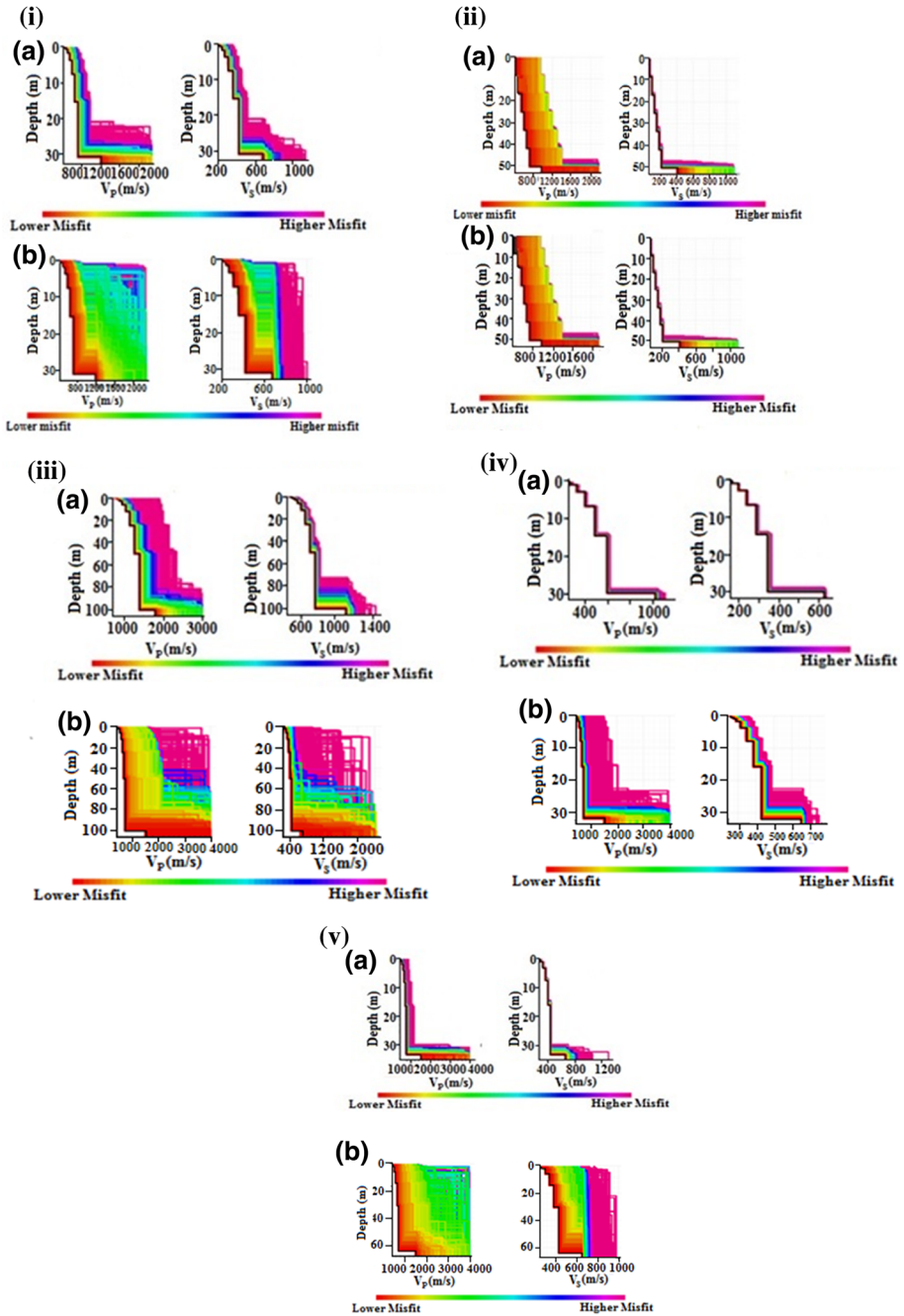


Fig. 4 Shear wave velocity profile estimated for the respective sites. Thick black solid line stands for best fitting model. **(i)** **a** From SPAC. **b** FK for ASSAM HOUSE. **(ii)** **a** From SPAC. **b** FK for NEHU. **(iii)** **a** From SPAC. **b** FK for RYLBANG. **(iv)** **a** From SPAC. **b** FK for POLO GROUND. **(v)** **a** From SPAC. **b** FK for LALCHAND BASTI

5.3 RYLBANG

5.3.1 From SPAC

This site is located on the outskirts of Shillong city. Importantly, there has been borehole drillings in the immediate neighborhood of this site. Owing to this, a priori information can be incorporated toward parameterization so as to decipher a reliable velocity structure underneath this site after computation of SPAC curves. On inverting the SPAC curves, the depth profiles obtained are displayed in Fig. 4(iii)a. For the surface layer having thickness of 4 m, V_S is estimated to be in the range of 385–525 m/s. Similarly, V_P is observed to be in the range of 600–700 m/s for the same layer. Going down the estimated profile, V_S is found to increase in regular intervals, and the same trend is also apparent in the estimates of V_P . For the bottom layer, V_S attains a value of 720 m/s.

5.3.2 From FK

The inversion of the dispersion curve corresponding to this array site produces the results as illustrated in Fig. 4(iii)b. The V_P values are estimated to be in the range of 400–645 m/s, while the V_S values are computed to be in the range of 290–415 m/s corresponding to the minimum misfit. The velocity to depth profile as attained in this site goes up to a depth of 51 m. The topmost layer yields an estimate of 290–310 m/s as V_S value.

5.4 POLO GROUND

5.4.1 From SPAC

As for this site, the shear wave velocity to depth profile has been estimated up to depth of 30 m, as illustrated in Fig. 4(iv)a. It is evident from the profile that the topmost layer reveals a shear wave estimate of 120 m/s. Toward the deeper formations, the value of V_S is found to increase up to 325 m/s. Similar trend in estimates of V_P values has also been observed. The V_P is found to be 300 m/s for the uppermost layer having thickness of 1 m. The corresponding dispersion curve yielded by the inversion is shown in the same figure.

5.4.2 From FK

The inversion results are demonstrated in Fig. 4(iv)b. The shear wave velocity models show some interesting estimates of V_P and V_S , respectively. So far, V_P values are concerned; they range from 445 to 680 m/s. Estimates of V_S values lie between 220 and 425 m/s. The inverted model shows velocity variations up to the depth of 30 m. As for the dispersion curves, the slowness rises with increase in frequency.

5.5 LALCHAND BASTI

5.5.1 From SPAC

Figure 4(v)a demonstrates the results from inversion of the observed SPAC curves. The uppermost layer which is of 3 m thickness shows a V_S value of 275 m/s, whereas the same layer gives 500 m/s as estimate of V_P value. The strata having higher thickness yields the

largest estimate of V_S value which is observed to be 410 m/s. Similarly, the corresponding value of V_P is estimated to be 700 m/s. Going down the profile, it is apparent that shear wave velocity increases as the depth of the profile too increases.

5.5.2 From FK

The inversion results for this array site are demonstrated in Fig. 4(v)b. The inverted V_P and V_S models have been constrained to the depth of 30 meters only due to lack of a priori information. The V_P values range between 750 and 1250 m/s, whereas the V_S values are observed to be in the range of 275–625 m/s up to the depth of 30 m. The velocity profiles show a constant rise as the depth section is increased corroborating surmises that velocity is dependent on depth.

6 Correlation with geophysical and geotechnical parameters

The estimated shear wave velocity models obtained through these different techniques are found to be compatible with each other. However, to emphasize validation, we have tried to correlate with available geophysical and geotechnical information. Accordingly, available geotechnical and geophysical information like borehole data, resistivity data and gravity data are considered as key inputs for correlation.

So far other geotechnical information is concerned; the report on resistivity profile available at Rajbhaban Area by Central Ground Water Board (CGWB) (2008) Shillong indicates higher resistivity values at depths of 20–30 m. Figure 5 demonstrates the results found in the report, with values ~ 2650–6500 Ohm-meters. This is also indicated in inset table in Fig. 5. As per Lay and Wallace (2001), higher values of resistivity implicate the

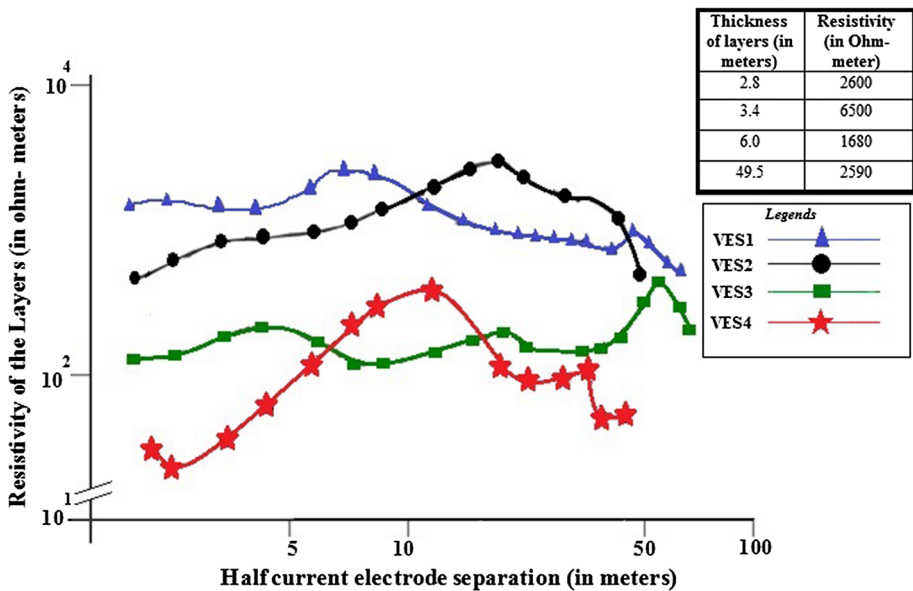


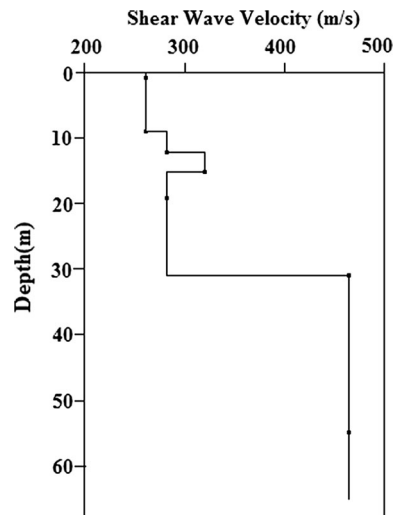
Fig. 5 Resistivity profile of the Rajbhaban area (after Central Ground Water Board 2008). In the bottom right corner, the corresponding resistivity values are provided for this site. Resistivity is provided against each layer in ohm-meter units. VES here refers to vertical electric sounding

existence of stiff soil strata, overlain by basement rock. In such cases, the shear wave velocity rises with growing compactness of the strata. RYLBANG is in immediate neighborhood of Rajbhaban area. As such, our estimates tally with these higher resistivity values.

Apart from this, there are instances of other geophysical investigations carried out in and around Shillong city. As for example, Geological Survey of India executed a planned program of geophysical investigations employing magnetic, resistivity, gravity, etc. in an area, covering 6 km² (GSI 1985; Dasgupta and Biswas 2000; Kalita 1998). As per their report, a zone of low resistivity and moderate gravity anomaly of 0.3 milligals exists in the NEHU campus which they attribute to localized region of carbonaceous phyllite up to the depth of 102 and 139 m. This region extends up to 3.2 km in Shillong area. This observation is found to be consistent with the derived shear wave velocity models in this work. Generally, areas yielding low resistivity are considered as low-velocity zones, i.e., shear wave velocity decreases with lower porosity and lower density, pertinent to stratum. The V_S values estimated by the inversion of the SPAC and the FK results as well, corresponding to this NEHU site, are observed to be relatively low, i.e., in the range of 150–300 m/s. However, toward the other side of this Shillong area, study of GSI (1985) inferred the abundance of metabasic rocks such as quartzite, phyllites having higher resistivity. Accordingly, the derived velocity model exhibits higher values of shear wave velocities in conformity with the results of geophysical investigation.

Further, we empirically determined shear wave velocities by (Imai and Tonochi 1982; Ohta and Goto 1978) incorporating geotechnical parameters in the form of N values from standard penetration test. These empirically obtained values are in excellent match with the estimates obtained through these inversion techniques. As for instance, the empirically determined shear wave velocity profile matches reasonably well with the models, obtained through the inversion for LALCHAND BASTI (see Fig. 6). V_S has been empirically estimated to be in the range of 250–455 m/s which is quite comparable to shear wave velocity models evaluated through inversion. Simultaneously, the geological map as well as the available borehole information is found to be in good agreement with the estimates

Fig. 6 Shear wave velocity profile for LALCHAND BASTI site estimated through empirical relationship. Depth is plotted along vertical axis, whereas along the horizontal axis, empirically computed shear wave velocities are provided



of V_P and V_S profiles as obtained by the inversion in the other array sites such as POLO GROUND and ASSAM HOUSE.

7 Discussions

In this study, we have made an attempt to assess the shallow shear wave velocity structure of Shillong city. Simultaneously, determination of subsurface V_P values to a lesser extent remains another target. To achieve these objectives, we have blended two different methodologies, namely spatial autocorrelation method and frequency wave number technique. The inverted profiles (V_S and V_P values) are separately determined from the SPAC curves and frequency wave number curves for the five sites. Velocity profiles so estimated are correlated with available geophysical information.

Inversion of the autocorrelation curves through SPAC and dispersion curves computed through FK Technique are accomplished to decipher shear wave velocity to depth profile at each of the array sites. Simultaneously, V_P profiles are also estimated to a reliable extent. It can be inferred that SPAC technique reveals coherency on lower side of frequency which has been agreed by many researchers (Cho et al. 2004; Cornou et al. 2003; Raptakis and Makra 2010; Boore and Asten 2008; Claprod and Asten 2010) albeit there are some striking differences in the studied range of frequencies pertaining to the different array sites (Okada 2006).

While deriving the shear wave velocity models, it is asserted that the incorporation of the litholog information greatly improves the results (Wathelet et al. 2005). Out of the five array sites, three sites (POLO GROUND, NEHU and LALCHAND BASTI) are aided by sufficient geotechnical information in the form of borehole data. Shear wave velocity model is derived for these three sites based on the available information. Because of the inadequacy of litholog information at two other sites (RYLBANG and ASSAM HOUSE), the shear wave velocity models are interpolated from the available litholog information pertaining to three sites. The computation of the estimated models through SPAC and frequency wavenumber technique is found to be quite similar for all the four sites, except RYLBANG. As observed in RYLBANG, inversion of dispersion curve computed through frequency wave number produces lower estimate of V_S and V_P values compared with the inverted model corresponding to the SPAC curves. It is already mentioned that this site is just situated 100 meters away from the highway. This underestimation of shear wave velocities may be related to the absence of coherent and energetic plane wave arrival at the sensors. Another plausible explanation of this may be the insufficiency of energy of ambient vibration wavefield resulting from the filtering effect of the layers.

Several researchers reported this rising trend of subsurface shear wave velocities (Wathelet 2004; Scherbaum et al. 2003). As shown in the work of Tokimatsu et al. (1992) and Tokimatsu (1997), it was postulated that there existed a mixing of fundamental and higher-mode dispersion curves, which would result in overestimation/underestimation of phase velocity estimates in the dispersion data and could remain undetected by the analyst's quality control. Even though, it cannot be completely ruled out that there may be an overestimation of shear wave velocities in the proposed ambient vibration model as obtained in RYLBANG, most likely it may be attributed to bias in the estimate of sediment/bedrock interface depth.

So far the incorporation of prior litholog information is concerned toward reliable modeling of shear wave velocity profiles, two sites namely, ASSAM HOUSE and LALCHAND BASTI, lack prior information of litholog. In these two particular sites, the

estimate of the sediment thickness is not well constrained than the absolute values of the velocity–depth model as observed in other three sites. Similar observation was also reported by Scherbaum et al. (2003).

The thickness variations underneath the arrays do significantly perturb the dispersion curves. As our assumption is based upon laterally consistent 1D model, we cannot rule out the possibility of our results being affected by it. Since the fundamental mode of Rayleigh wave is taken resulting from vertical component in all the inversion processes, there is every possibility that higher modes of surface waves can also be present in ambient vibrations, as observed by Tokimatsu (1997). On the other hand, some small contribution of higher modes at higher frequencies may occur, as indicated by Asten et al. (2004). Therefore, the derived shear wave velocity models and V_P values, to a lesser extent, are constrained by adoption of the vertical component only, corresponding to these five array sites. However, it can be laid with emphasis that the derivations of shear wave velocity model for each respective site are quite substantiated by each of these techniques.

Apart from deriving shear wave velocity models through these techniques, we have performed a correlation analysis of the obtained models with available geotechnical and geophysical information. As for NEHU site, the inverted model is affirmed by resistivity values; similar is the case with RYLBANG site. Additionally, the empirically determined shear wave velocity profiles by us, following Ohta and Goto (1978), are in agreement with the computed models. Again, we have validated the shear wave velocity estimates through comparison of identical works by different researchers as enlisted in Table 6. Though, in many of the cases, the procedures adopted by them are different; but the ultimate goal was to find the shear wave velocities. While enlisting their works, it is kept in mind that the shear wave velocity estimates must correspond to the same lithology irrespective of the geographic location of the sites. The values yielded by these works tally well with the computed shear wave velocities for this study region. Meanwhile, it is observed that all the SPAC curves exhibit a decaying pattern of the autocorrelation ratios for higher band of frequencies. Similar trends are found in the works of several researchers, e.g., Wathelet

Table 6 Comparison of shear wave velocities from different literatures

References	Site geology	Computed velocity profiles, V_S	In this study
Clappord and Asten (2010)	Quaternary and tertiary sediments	400–500 m/s within 0–50 m	
Chávez-García et al. (2006)	Sediments with clayey soil	530 m/s at 35 m; 700 m/s at 78 m	
García-Jerez et al. (2007)	Similar	250–750 m/s up to 200 m depth	
Roberts and Asten (2008)	Quaternary sediments	200–500 m/s	Average 250–650 up to 50 depth
Rayhani et al. (2008)	Quaternary sediments	100–600 m/s up to 35 m	
Rayhani et al. (2008)	Same	200–500 up to depth 200 m	
Louie (2001)	Quaternary sediments	200–600 m/s	
Asten (2006)	Sediments	300–800 m/s up to 280 m depth	

et al. (2004), Bard (2004), Bettig et al. (2001) and Raptakis and Makra (2010). However, the stratification, observed in the velocity profiles estimated by these techniques, matches quite well with the stratification of the sites POLO GROUND, RYLBANG and NEHU as observed in the litholog.

Although we did implement these two techniques entailing different working principles, each of them is endowed with pros and cons. For example, SPAC procedure is fit for spatial and time coherent signals, reliably inferring one-dimensional velocity estimates with moderate impedance contrast. On the other hand, FK is found to suitably yield dispersion curves for sites which are characterized by sharp contrast and more plane wave arrivals. Since our study area is characterized by sharp to moderate contrast varying from site to site, this motivated us to adopt the joint inversion of dispersion curves yielded by both these methods to attain converging results.

The results have the useful impact in understanding the subsurface soil and in estimating seismic hazard of the region. The shear wave velocity estimates prove to be a vital input for geo-engineers, civil engineers as well as policy makers. Based on these estimates, it will be easier to build up a hazard map for the entire city. This will in other way help designers to find low-velocity zones and hence build earthquake resistant buildings, thereby mitigating the seismic hazard for a large impending earthquake. A further extension to a 2D and 3D model of the S-wave velocity profile obtained in this study would ease improved knowledge of the interior of the depth profiles which would be future course of action.

8 Conclusion

In this work, we show the analysis of ambient vibrations, recorded by seismic arrays installed in Shillong city in order to attain inverted shear wave velocity models. By adopting two robust methods, we have tried to retrieve the dispersion characteristics from recorded ambient vibrations. In this study, we have focused mostly on the vertical components of the ambient vibrations. The combined application of these two techniques allowed us to arrive at a suitable shear wave velocity model compatible to the study region (Shillong city).

- (a) The analysis carried out in this work has shown that it is possible to derive a velocity model of the S-wave velocity structure for the study area by means of low-cost measurements of ambient noise.
- (b) Our results are consistent with other available data.
- (c) The computed V_S values up to depth of 30 m are found to be in the range of 275–375 m/s.
- (d) These attained values of V_S in most of the sites imply prevalence of low-velocity zones at some pocket areas, as supported by formidable evidence of site geology and geotechnical information.

Further numerical and experimental works are now in process in order to give a clear assessment of the obtained results. In other words, more input from seismic reflection and refraction studies would enhance the reliability of the findings. Despite lack of priori information of V_P and V_S values at two of the sites, we could reliably retrieve the velocity to depth profiles.

References

- Aki K (1957) Space and time spectra of stationary waves with special reference to micro tremors. *Bull. Earth. Res. Inst. Univ. Tokyo* 35:415–456
- Asten MW (2006) On bias and noise in passive seismic data from finite circular array data processed using SPAC methods. *Geophysics* 71(6):V153–V162
- Asten MW, Dhu T, Lam N (2004) Optimized array design for microtremor array studies applied to site classification; comparison of results with SCPT logs. In: *Proceedings of the 13th World Conference on Earthquake Engineering*, Vancouver, Canada, Paper No. 2903
- Bard PY (2004) The SESAME project: an overview and main results. In: *13th World Conference on Earthquake Engineering*, August 2004, Vancouver, Canada, paper No. 2207
- Bettig B, Bard PY, Scherbaum F, Riepl J, Cotton F, Cornou C, Hatzfeld D (2001) Analysis of dense array noise measurements using the modified spatial auto-correlation method (SPAC): application to the Grenoble area. *Boll Geofis Teor Appl* 42:281–304
- Biswas R, Baruah S (2011) Site response estimation by Nakamura method: Shillong City, Northeast India. *Memoir of the Geophysical Society of India*, No. 77, 173–183
- Biswas R, Baruah S (2015) Non-linear earthquake site response analysis: a case study in Shillong City. *IJEHRM* (3:4)
- Biswas R, Baruah S (2016) Shear wave velocity estimates through combined use of two passive techniques of a tectonically active area. *Acta Geophys* (64/6)
- Biswas R, Bora DK, Baruah S, Kalita A, Baruah S (2013a) The effects of attenuation and site on the spectra of microearthquakes in the Shillong Region of Northeast India. *Pure Appl Geophys* 170(11):1833–1848
- Biswas R, Bora DK, Baruah S (2013b) Influence of attenuation and site effects in the spectra of micro earthquakes originating in Shillong City, NER, and India. *Acta Geophys* 61:886–904
- Biswas R, Baruah S, Baruah S (2014) A brief overview of site response estimation techniques. *Mistral Services: Italy*, ISBN: 978-88-98161-25-6
- Biswas R, Bora DK, Baruah S (2015) Mapping sediment thickness in Shillong City of northeast India. *J Earthq.* <https://doi.org/10.1155/2015/572619>
- Biswas R, Bora N, Baruah S (2018) Frequency dependent site response inferred from microtremors accompanied by ambient noise. *Phys Astron Int J* 2(4):273–277. <https://doi.org/10.15406/paij.2018.02.00098>
- Boore DM, Asten MW (2008) Comparisons of shear-wave slowness in the Santa Clara Valley, California, using blind interpretations of data from invasive and noninvasive methods. *Bull Seismol Soc Am* 98(4):1983–2003
- Borcherdt RD (1970) Effects of local geology on ground motion near San Francisco Bay. *Bull Seismol Soc Am* 60:29–61
- Bozdogan E, Kocaoğlu AH (2005) Estimation of site amplification from shear wave velocity profiles in Yesilyurt and Avcılar, Istanbul by frequency-wavenumber analysis of microtremors. *J Seismol* 9:87–98
- Campbell KW (1976) A note on the distribution of earthquake damage in Long Beach, 1933. *Bull Seismol Soc Am* 86:1001–1006
- Chattopadhyaya N, Hashimi S (1984) The Sung valley alkaline ultramafic carbonatite complex, East Khasi Hills district, Meghalaya. *Rec Geol Surv India* 113:24–33
- Chávez-García FJ, Rodríguez M, Stephenson WR (2006) Subsoil structure using SPAC measurements along a line. *Bull Seismol Soc Am* 96(2):729–736
- Cho I, Tada T, Shinozaki Y (2004) Suggestion and theoretical evaluations on the performance of a new method to extract phase velocities of Rayleigh waves from microtremor seismograms obtained with a circular array. In: *13th World Conference on Earthquake Engineering*, Paper No. 647
- Claprod M, Asten MW (2007a) Use of SPAC, HVSr and strong motion analysis for site hazard study over the Tamar Valley in Launceston, Tasmania. In: *Earthquake Engineering in Australia Conference*
- Claprod M, Asten MW (2007b) Combined use of SPAC, FK and HVSr microtremor survey methods for site hazard study over the Tamar Valley in Launceston, Tasmania. In: *Extended abstracts of the ASEG 19th Geophysical Conference and Exhibition*, Perth
- Claprod M, Asten MW (2010) Statistical validity control on SPAC microtremor observations recorded with a restricted number of sensors. *Bull Seismol Soc Am* 100(2):776–791
- Cornou C, Bard P-Y, Dietrich M (2003) Contribution of dense array analysis to the identification and quantification of basin-edge-induced waves, part I: methodology. *Bull Seismol Soc Am* 93:2604–2623
- Dasgupta A, Biswas A (2000) *Geology of Assam*. Geol Soc India, Bangalore

- Di Giulio G, Cornou C, Ohrnberger M, Wathelet M, Rovelli A (2006) Deriving wavefield characteristics and shear velocity profiles from two dimensional small aperture arrays analysis of ambient vibrations in a small size alluvial basin, Colfiorito, Italy. *Bull Seismol Soc Am* 96:1915–1933
- Fäh D, Kind F, Giardini D (2003) Investigation of local S-wave velocity structures from average H/V ratios, and their use for the estimation of site effects. *J Seismol* 7:449–467
- Garcia-Jerez A, Navarro M, Alcalá FJ, Luzon F, Perez Ruiz JA, Enomoto T, Vidal F, Ocana E (2007) Shallow velocity structure using joint inversion of array and h/v Spectral ratio of ambient noise, The case of Mula Town (SE of Spain). *Soil Dyn Earthq Eng* 27:907–919
- GSI (1985) Geology mapping in greater Shillong area, Meghalaya. *Memoir Geol. Surv. India*
- Hartzell SH, Liu P, Mendoza C (1996) The 1994 Northridge, California earthquake: investigation of rupture velocity, rise time, and high-frequency radiation. *J Geophys Res* 101, 20, 091–20,108
- Imai T, Tonouchi K (1982) Correlation of N-value with S-wave velocity and shear modulus. In: *Proceedings 2nd European Symposium on Penetration Testing Amsterdam*, pp 57–72
- Kalita BC (1998) Ground water prospects of Shillong Urban Agglomerate. Unpublished report. Central Ground Water Board, Meghalaya
- Kassaras I, Kalantoni D, Benetatos Ch, Kaviris G, Michalaki K, Sakellariou N, Makropoulos K (2015) Seismic damage scenarios in Lefkas old town (W. Greece). *Earth Eng. Bull.* <https://doi.org/10.1007/s10518-015-9789-z>
- Kayal JR (2008) *Microearthquake seismology and seismotectonics of South Asia*. Springer, Berlin, pp 273–275
- Kayal JR, Arefiev SS, Baruah S, Hazarika D, Gogoi N, Kumar A, Chowdhury SN, Kalita S (2006) Shillong Plateau Earthquakes in northeast India region: complex tectonic model. *Curr Sci* 91:109–114
- Köhler A, Ohrnberger M, Scherbaum F, Wathelet M, Cornou C (2007) Assessing the reliability of the modified three-component spatial autocorrelation technique. *Geophys J Int* 168:779–796
- Kvaerna T, Ringdahl F (1986) Stability of various fk-estimation techniques. In: *Semiannual Technical Summary*, 1 October 1985–31 March 1986. In: *NORSAR Scientific Report*, 1-86/87, Kjeller, Norway, 29-40
- Lay T, Wallace TC (2001) *Modern global seismology*. Academic Press, San Diego
- Louie LN (2001) Faster, better: shear wave velocity to 100 meters depth from refraction microtremor arrays. *Bull Seismol Soc Am* 91:347–364
- Mitra S, Mitra C (2001) Tectonic setting of the precambrians of the northeastern India, Meghalaya Plateau, and area of Shillong group of rocks. *Geol Surv India Spec Publ* 64:653–658
- Ohrnberger M, Schissle E, Cornou C, Wathelet M, Savvaidis A, Scherbaum F, Jongmans D, Kind F (2004a) Microtremor array measurements for site effect investigations: comparison of analysis methods for field data crosschecked by simulated wavefields, Paper No. 0940, XIII World conference on Earthquake Engineering, Vancouver, BC, Canada, 1–6 August 2004
- Ohrnberger M, Scherbaum F, Krüger F, Pelzing R, Reamer S-K (2004b) How good are shear wave velocity models obtained from inversion of ambient vibrations in the Lower Rhine Embayment (NW-Germany). *Boll Geof Teor Appl* 45(3):215–232
- Ohta Y, Goto N (1978) Empirical shear wave velocity equations in terms of soil characteristics soil indexes. *Earthq Eng Struct Dyn* 6:167–187
- Okada H (2006) Theory of efficient array observations of microtremors with special reference to the SPAC method. *Explor Geophys* 37(1):73–84
- Papadopolou-Vrynioti K, Bathrellos GD, Skilodimou HD, Kaviris G, Makropoulos K (2013) Karst collapse susceptibility mapping considering peak ground acceleration in a rapidly growing urban area. *Eng Geol* 158:77–88
- Pavlou K, Kaviris G, Chousianitis K, Drakatos G, Kouskouna V, Makropoulos K (2013) Seismic hazard assessment in Polyphyto Dam area (NW Greece) and its relation with the unexpected earthquake of 13 May 1995 ($M_s = 6.5$, NW Greece). *Nat Hazards Earth Syst Sci*
- Picozzi M, Parolai S, Albarello D (2005) Statistical analysis of noise horizontal-to-vertical spectral ratios (HVSR). *Bull Seismol Soc Am* 95(5):1779–1786
- Rao JM, Purnachandra Rao GVS (2008) Geology, geochemistry and palaeomagnetic study of Cretaceous Mafic Dykes of Shillong Plateau and their evolutionary history Indian Dykes. *Geochem Geophys Geomorphol* 589–607
- Raptakis D, Makra K (2010) Shear wave velocity structure in western Thessaloniki (Greece) using mainly alternative SPAC method. *Soil Dyn Earthq Eng* 30:202–214
- Rayhani MHT, El Naggat MH, Tabatabai SH (2008) Nonlinear analysis of local site effects on seismic ground response in the Bam earthquake. *Geotech Geol Eng* 21(1):91–100
- Roberts J, Asten MW (2008) A study of near source effects in array-based (SPAC) microtremor surveys. *Geophys J Int* 174(1):159–177. <https://doi.org/10.1111/j.1365-246X.2008.03729.x>

- Sambridge M (1999a) Geophysical inversion with a neighborhood algorithm-I. Searching a parameter space. *Geophys J Int* 138:479–494
- Sambridge M (1999b) Geophysical inversion with a neighborhood algorithm-II. Appraising the ensemble. *Geophys J Int* 138:727–746
- Sar SN (1973) An interim report on ground water exploration in the Greater Shillong area, Khasi Hills District, Meghalaya: Memo report, Central Ground Water Board
- Scherbaum F, Hinzen KG, Ohrnberger M (2003) Determination of shallow shear wave velocity profiles in the Cologne, Germany area using ambient vibrations. *Geophys J Int* 152:597–612
- Seligson CD (1970) Comments on high-resolution frequency wavenumber spectrum. *Anal Proc IEEE* 58:947–949
- SESAME (2004) Guidelines for the implementation of the H/V spectral ratio technique on ambient vibrations measurements, processing and interpretation. SESAME European Research Project WP12-Deliverable D23.12
- Srinivasan P, Sen S, Bandopadhyaya PC (1996) Study of variation of Paleocene-Eocene sediments in the shield areas of Shillong Plateau. *Rec Geol Surv India* 129:77–78
- Tokimatsu K (1997) Geotechnical site characterization using surface waves. In: Ishihara (ed) *Proc. 1st Intl. Conf. Earthquake Geotechnical Engineering*. Balkema, pp 1333–1368
- Tokimatsu K, Shinzawa K, Kuwayama S (1992) Use of short-period micro tremors for V_s profiling. *J Geotech Eng* 118(10):1554–1558
- Wathelet M, Jongmans D, Ohrnberger M (2004) Surface-wave inversion using a direct search algorithm and its application to ambient vibration measurements. *Near Surf Geophys* 2:211–221
- Wathelet M, Jongmans D, Ohrnberger M (2005) Direct inversion of spatial autocorrelation curves with the neighborhood algorithm. *Bull Seismol Soc Am* 95(5):1787–1800. <https://doi.org/10.1785/0120040220>
- Williams RA, Stephenson WJ, Odum JK (2003) Comparison of P-and S-wave velocity profiles obtained from surface seismic refraction/reflection and downhole data. *Tectonophysics* 368(1):71–88
- Woods JW, Lintz PL (1973) Plane waves at small arrays. *Geophysics* 38:1023–1041
- Yamanaka H (1998) Geophysical explorations of sedimentary structures and their characterization. In: Irikura K, Kudo K, Okada H, Sasatani T (eds) *Second international symposium on the effects of surface geology on seismic motion*, vol 1, pp 15–33
- Yamanaka H, Dravinski M, Kagami H (1993) Continuous measurements of microtremors on sediments and basement in Los Angeles, California. *Bull Seismol Soc Am* 83–5:1595–1609
- Yamanaka H, Takemura M, Ishida H, Niwa M (1994) Characteristics of long-period microtremors and their applicability in exploration of deep sedimentary layers. *Bull Seismol Soc Am* 84–6:1831–1841